Available online at www.sciencedirect.com
SCIENCE DIRECT®
Computers and Chemical Engineering 29 (2004) 225–241
Computers & Chemical Engineering
www.elsevier.com/locate/compchemeng

Feedback control of surface roughness of GaAs (0 0 1) thin films using kinetic Monte Carlo models

Yiming Lou, Panagiotis D. Christofides*

Department of Chemical Engineering, University of California, Los Angeles, CA 90095, USA

Received 20 August 2003; received in revised form 2 March 2004; accepted 20 July 2004
Available online 11 September 2004

Abstract

In this work, we follow the methodology presented in Lou and Christofides [Estimation and control of surface roughness in thin-film growth using kinetic Monte-Carlo models, Chem. Eng. Sci. 58 (2003a) 3115–3129] to study estimation and control of surface roughness of gallium arsenide (GaAs) (0 0 1) thin films during deposition in a horizontal-flow quartz reactor using triisobutylgallium (TIBGa) and tertiarybutylarsine (TBAs) as precursors with H_2 as the carrier gas. The adsorption of TIBGa onto the surface and the migration of Ga atoms on the surface are considered as the two rate-limiting steps in the film growth and are explicitly modeled within a kinetic Monte Carlo simulation framework. The energy barrier and the pre-exponential factor of the migration rate of Ga atoms on the surface used in the simulations are initially determined by fitting the simulation results to experimental data reported in Law et al. [Analysis of the growth modes for gallium arsenide metalorganic vapor-phase epitaxy, J. Appl. Phys. 88 (2000) 508–512]. Then, a roughness estimator is constructed that allows computing estimates of the surface roughness of the GaAs thin films at a time-scale comparable to the real-time evolution of the process using discrete on-line roughness measurements. The estimator involves a kinetic MC simulator based on multiple small-lattice models, an adaptive filter used to reduce roughness stochastic fluctuations and an error compensator used to reduce the error between the roughness estimates and the roughness measurements. The roughness estimates are fed to a proportional–integral (PI) feedback controller which is used to control the surface roughness to a desired level by manipulating the substrate temperature. Application of the proposed estimator/controller structure to the process model based on a large-lattice kinetic Monte Carlo simulator demonstrates successful regulation of the surface roughness to the desired level. The proposed approach is shown to be superior to PI control with direct use of the discrete roughness measurements. The reason being that the available measurement techniques do not provide measurements at a frequency that is comparable to the time-scale of the dominant film growth dynamics.

Keywords: Feedback control; Surface roughness; Kinetic Monte Carlo models; Gallium arsenide thin films; State estimation

1. Introduction

Deposition of thin films from gas-phase precursors is of importance in electronic chip manufacture. Modern integrated circuit technology depends strongly on the uniformity and microstructure of thin films of advanced materials (Granneman, 1993). Due to the increasingly stringent requirements on the quality of such films, including uniformity, composition, microstructure, and the desire to improve productivity by increasing wafer dimensions and reducing product variability, real-time feedback control of thin-film deposition becomes increasingly important. These trends have motivated significant research efforts on feedback control of film deposition processes to control film composition (e.g., Ni et al., 2004) and to control film spatial uniformity in rapid thermal (e.g., Baker & Christofides, 1999; Theodoropoulou, Adomaitis, & Zafiriou, 1999) and plasma-enhanced chemical vapor deposition (e.g., Armaou & Christofides, 1999). From a control point of view, film spatial uniformity control is a distributed control problem that can be addressed on the basis of continuum-type transport-reaction models by using controller design methods for nonlinear parabolic partial dif-

* Corresponding author.
Tel.: +1 310 794 1015; fax: +1 310 206 4107.
E-mail addresses: ylou@seas.ucla.edu (Y. Lou), pdc@seas.ucla.edu (P.D. Christofides).

0098-1354/$ – see front matter © 2004 Elsevier Ltd. All rights reserved.
doi:10.1016/j.compchemeng.2004.07.006

Nomenclature

E_s	energy barrier associated with migration due to surface effect (eV)
E_n	energy barrier associated with migration due to nearest-neighbor interactions (eV)
h	Planck's constant (J s)
k_B	Boltzmann's constant (J/K)
K	filter gain
K_c	controller gain (K/Å)
K_e	compensator gain (s^{-1})
r	surface roughness (Å)
Δt	life time of one MC event (s)
T	temperature (K)

Greek letters

ϵ	tolerance (Å)
ν_0	pre-exponential factor (s^{-1})
τ_I	filter time constant (s)
τ_c	controller time constant (s)

ferential equations (PDEs) (Christofides & Daoutidis,1997; Baker & Christofides, 2000; Christofides, 2001).

However, to control microscopic film properties such as surface roughness of the ultra-thin films, it is important to understand and to model the dependence of film microstructure evolution on macroscopic (controllable) process variables. This need has motivated extensive research on the development of fundamental mathematical models describing thin-film growth and its interactions with the surrounding gas. From a microscopic point of view, the rates of surface microprocesses (e.g., adsorption, desorption, migration and reaction) are key factors that determine thin-film microstructure and composition. These rates depend strongly on macroscopic process parameters like precursor concentration and substrate temperature, to name a few. Kinetic Monte Carlo (MC) simulation provides a framework for modeling the effect of macroscopic process variables on thin-film microstructure.

Mathematically, kinetic MC simulation methods provide an unbiased realization of the master equation (Gillespie, 1976; Van Kampen, 1992), which is a stochastic partial differential equation describing the evolution of the probability that the thin film is at a certain microconfiguration. Kinetic MC simulation results are consistent to the master equation in the sense that the simulation algorithms are derived based on the same assumptions employed in the derivation of the master equation (Gillespie, 1977). Kinetic MC simulation can be used to predict average properties of the thin film (which are of interest from a control point of view, like, e.g., surface roughness), by explicitly accounting for the microprocesses that directly shape thin-film microstructure. Since a kinetic MC simulation run constitutes a realization of a stochastic process, simulation results from different simulation runs are not identical. However, by averaging the simulation results from different runs, the averaged properties of the thin film converge to the values obtained from the solution of the master equation.

The accuracy of solutions from one kinetic MC simulation run depends on the size of the lattice used in the simulation which, in turn, determines the computational requirements of the simulation. Specifically, the larger the lattice, the smaller the fluctuations contained in the simulation results. However, the computational requirements of kinetic MC simulators, based on high-order lattice models, make their direct use in an on-line feedback control scheme impossible. Motivated by this, recent research efforts have focused on the construction of estimators and controllers, which can be implemented in real-time with reasonable computing power, for thin-film surface roughness and growth rate regulation based on kinetic MC simulators using multiple small-lattice models (Lou & Christofides, 2003a,b). Other approaches have also been developed to: (a) identify linear models from outputs of kinetic Monte Carlo simulators and perform controller design by using linear control theory (Siettos, Armaou, Makeev, & Kevrekidis, 2003) and (b) construct reduced-order approximations of the master equation (Gallivan & Murray, 2003).

Gallium arsenide (GaAs) is an important compound semiconductor that has many applications including light-emitting diodes, microwave devices, broadband communications, and space solar cells (Fu, Li, & Hicks, 2000). The GaAs thin films can be deposited by either molecular-beam epitaxy (MBE) (e.g., Vanhove, Lent, Pukite, & Cohen, 1983) or metal-organic chemical vapor deposition (MOCVD) (e.g., Tirtowidjojo & Pollard, 1988; Law, Li, Begarney, & Hicks, 2000). Extensive experiment has been done to study the surface roughness of GaAs thin films under different deposition conditions using reflection high-energy electron diffraction (RHEED) (e.g., Shitara et al., 1992a,b), scanning tunnelling microscopy (STM) (e.g., Kasu & Kobayashi, 1997; Law et al., 2000) and atomic force microscopy (AFM) (e.g., Tejedor, Šmilauer, Roberts, & Joyce, 1999).

Extensive research has also been carried out to study the GaAs thin-film growth by using kinetic Monte Carlo simulations. Monte Carlo simulation for GaAs thin-film growth by MBE was first performed by Shitara et al. (1992a,b). In this study, the authors explicitly modeled the adsorption onto the surface and migration of Ga atoms because these rate-limiting steps determine film growth and microstructure. The effects of all other surface processes (As-related surface processes and surface reconstruction) were incorporated into the model by computing an "effective" energy barrier to Ga surface migration rate based on experimental results. A more detailed kinetic Monte Carlo model (which considers the kinetics of both Ga and As atoms) was recently developed by Ishii and Kawamura (1999). Furthermore, a theoretical investigation of the adsorption and migration on GaAs surface using density functional theory was performed in Shiraishi (1996).

By using Monte Carlo models to simulate the formation of GaAs thin films, phenomena such as atomic nucleation, growth, island formation and structural transformation can be studied (e.g., Ito & Shiraisho, 1996; Meng & Weinberg, 1996; Itoh, Bell, Joyce, & Vvedensky, 2000; Shiraishi, 2001).

In this work, we follow the methodology presented in Lou and Christofides (2003a) to study estimation and control of surface roughness of GaAs (0 0 1) thin films during deposition in a horizontal-flow quartz reactor using triisobutylgallium (TIBGa) and tertiarybutylarsine (TBAs) as precursors and H_2 as the carrier gas. The adsorption of TIBGa onto the surface and the migration of Ga atoms on the surface are considered as the two rate-limiting steps in the film growth and are explicitly modeled within a kinetic Monte Carlo simulation framework. The energy barrier and the pre-exponential factor of the migration rate of Ga atoms on the surface used in the simulations are initially determined by fitting the simulation results to the experimental data reported by Law et al. (2000). Then, a roughness estimator is constructed that allows computing estimates of the surface roughness of the GaAs thin films at a time-scale comparable to the real-time evolution of the process using discrete on-line roughness measurements. The estimator involves a kinetic MC simulator based on multiple small-lattice models, an adaptive filter used to reduce roughness stochastic fluctuations and an error compensator used to reduce the error between the roughness estimates and the roughness measurements. The roughness estimates are fed to a proportional–integral (PI) feedback controller which is used to control the surface roughness to a desired level by manipulating the substrate temperature. Application of the proposed estimator/controller structure to the process model based on a large-lattice kinetic Monte Carlo simulator demonstrates successful regulation of the surface roughness to the desired level. The proposed approach is shown to be superior to PI control with direct use of the discrete roughness measurements. The reason is that the available measurement techniques do not provide measurements at a frequency that is comparable to the time-scale of the dominant film growth process dynamics.

2. Surface microstructure model for GaAs thin-film growth

We use the Monte Carlo model presented in Shitara et al. (1992b) to model the surface microprocesses during the growth of GaAs thin films. Although the GaAs thin film is a two-component film, the simulation only considers the adsorption and migration of Ga atoms because in an As-rich environment (which is the case for the process considered in this work), As-related kinetics are not rate-limiting and can be incorporated into the model by using an "effective" energy barrier to model the surface migration rate of Ga atoms. We note that the MC model in Shitara et al. (1992b) is for growth of GaAs thin film by MBE. However, based on the experimental results presented in Law et al. (2000), the rate-limiting processes in GaAs thin-film growth by MOCVD are the same to those in GaAs thin-film growth by MBE. Therefore, we can use the same model but with a different "effective" energy barrier for the migration rate of Ga atoms, to model GaAs thin-film growth by MOCVD.

In Section 2.1, we describe the process of GaAs thin-film growth by MOCVD considered in this study and show the similarity of the rate-limiting processes involved in this process to that in GaAs thin-film growth by MBE.

2.1. Process description

For purposes of this study, the MOCVD growth of GaAs occurs in a horizontal-flow quartz reactor, with precursors of triisobutylgallium (TIBGa)/tertiarybutylarsine (TBAs) and the carrier gas is H_2. The pressures of the precursors and of the carrier gas are 0.25 mTorr for TIBGa, 25 mTorr for TBAs and 20 Torr for H_2. Therefore, the growth occurs in an As-rich environment. Under these precursor pressures, the growth rate is $0.5\,\mu$m/h, which is independent of the substrate temperature when the substrate temperature varies from 825 to 900 K (Law et al., 2000).

During the deposition, the precursor molecules TIBGa and TBAs first adsorb onto the surface. The TIBGa molecules adsorb onto the surface sites occupied by As atoms and TBAs molecules adsorb onto the surface sites occupied by Ga atoms. Upon adsorption of precursor molecules onto the surface, surface reactions occur; specifically, Ga atoms and As atoms are generated by the decompositions of TIBGa and TBAs on the surface. The butyl groups from the decomposition of TIBGa or TBAs desorb rapidly back to the gas phase at the high temperatures considered in this study (750–950 K) (Cui, Ozeki, & Ohashi, 1998). Due to the fact that the pressure of TBAs is much higher than that of TIBGa (the As/Ga ratio is 100), the diffusing species controlling the epitaxial growth is the Ga atoms (Law et al., 2000).

The rate-limiting steps are the adsorption of TIBGa and the migration of Ga atoms. Because the decomposition of TIBGa is very fast, the adsorption of TIBGa onto the surface can be simply modeled by the adsorption of Ga atoms onto the surface. Therefore, to model the surface microstructure, we only consider adsorption of Ga atoms and migration of surface Ga atoms.

During deposition, Ga atoms must adsorb onto surface sites occupied by As atoms and As atoms must adsorb onto surface sites occupied by Ga atoms. Because the As/Ga ratio is very high (about 100), we assume that right after a Ga atom adsorbs onto the surface, it is immediately covered by an As atom. Therefore, the same site is immediately available for the adsorption of next Ga atom. Consequently, all the surface sites are available for adsorption of Ga atoms at all times and the adsorption rate of Ga atoms is treated as site-independent. Furthermore, when the growth rate is fixed, the adsorption

rate on each surface site is a constant:

$$w_a = F \tag{1}$$

The migration rate of each surface Ga atom depends on its local environment. Assuming only first nearest-neighbor interactions, the migration rate of a surface Ga atom from a surface site with n first nearest-neighbors is (Shitara et al., 1992a,b):

$$w_m(n) = \nu_0 \exp\left(-\frac{E_s + nE_n}{k_B T}\right) \tag{2}$$

where E_s is the energy barrier associated with migration due to surface effects, E_n is the energy barrier associated with migration due to nearest-neighbor interactions, k_B is the Boltzmann's constant, and ν_0 is the pre-exponential factor.

2.2. Derivation of surface microstructure model based on probability theory

The formation of GaAs thin films by adsorption and migration of Ga atoms is a stochastic process because: (a) the exact time and location of the occurrence of one specific surface micro-process (adsorption or migration) are unknown, and (b) the probability (rate) with which each surface micro-process may occur is only available. Therefore, the surface evolution model should be established based on probability theory. A rigorous derivation of kinetic MC algorithm for chemical reactions was first carried out in Gillespie (1976). In the present study, we follow the same methodology to derive the Monte Carlo model for surface microstructure of GaAs thin-film growth by MOCVD.

Specifically, we treat the surface micro-processes (adsorption and migration of Ga atoms) as Poisson processes, which means that the following assumptions are made (e.g., Melsa & Sage 1973; Feller 1975; Gillespie, 1976; Fichthorn & Weinberg, 1991).

Assumption 1. The probability that k events occur in the time interval $(t, t+T)$ is independent of t.

Assumption 2. The probability that k events occur in the time interval $(t, t+T)$ is independent of the number of events occurring in any non-overlapping time interval.

Assumption 3. The probability that an event occurs in an infinitesimal time interval $(t, t+\mathrm{d}t)$ is equal to $W\,\mathrm{d}t$ (where W is the mean count rate of the event), and the probability of more than one event occurring in an infinitesimal time interval is negligible.

Based on these three assumptions, the time evolution of probabilities that the surface is in one specific configuration can be derived. The configuration of a surface is characterized as the height of each surface atom at each surface site. If $P(\alpha, t)$ represents the probability that the system is in configuration α at time t, based on Assumptions 2 and 3, we have the following equation for $P(\alpha, t+\mathrm{d}t)$:

$$P(\alpha, t+\mathrm{d}t) = P(\alpha, t)P_{0\alpha} + \sum_{\beta} P(\beta, t)P_{1\beta} \tag{3}$$

where $P_{0\alpha}$ is the probability that no event occurs in the time interval $(t, t+\mathrm{d}t)$ given that the surface is in configuration α at t, $P(\beta, t)$ is the probability that the surface is in configuration β at t and $P_{1\beta}$ is the probability that one event occurs in the time interval $(t, t+\mathrm{d}t)$ given that the surface is in configuration β at t, and the occurrence of this event results to a transition from configuration β to configuration α.

$P_{0\alpha}$ and $P_{1\beta}$ have the following expressions (a detailed proof can be found in Gillespie (1992)). Specifically,

$$P_{0\alpha} = 1 - \sum_{\beta} W_{\beta\alpha}\,\mathrm{d}t \tag{4}$$

where $W_{\beta\alpha}\,\mathrm{d}t$ is the probability that an event occurs in the time interval $[t, t+\mathrm{d}t)$ which results in a transition from configuration α to a configuration β, therefore, $\sum_{\beta} W_{\beta\alpha}\,\mathrm{d}t$ is the probability that any one event occurs in the time interval $(t, t+\mathrm{d}t)$ provided that the surface configuration is α at t. Moreover,

$$P_{1\beta} = W_{\alpha\beta}\,\mathrm{d}t \tag{5}$$

where $W_{\alpha\beta}\,\mathrm{d}t$ is the probability that an event happens in the time interval $[t, t+\mathrm{d}t)$ and the occurrence of this event results to a transition from configuration β to configuration α.

By substituting Eqs. (4) and (5) into Eq. (3) and taking the limit $\mathrm{d}t \to 0$, we obtain a differential equation describing the time evolution of the probability that the surface is in configuration α:

$$\frac{\mathrm{d}P(\alpha, t)}{\mathrm{d}t} = \sum_{\beta} P(\beta, t)W_{\alpha\beta} - \sum_{\beta} P(\alpha, t)W_{\beta\alpha} \tag{6}$$

Eq. (6) is the so-called "master equation" (ME) for a stochastic process. The ME has a simple, linear structure, however, it is difficult to write the explicit form of Eq. (6) for any realistic system because the number of the possible states (configuration) is extremely large for most systems of a realistic size. For example, for a system with 10×10 sites and a maximum height of 1, the number of configurations is $2^{100} \approx 10^{30}$. This makes the direct solution of Eq. (6), for any system of meaningful size, using numerical methods for integration of ordinary differential equations (e.g., Runge–Kutta) impossible.

Monte Carlo techniques provide a way to obtain unbiased realizations of a stochastic process, which is consistent with the ME. The consistency of the Monte Carlo simulation to the ME is based on the fact that in a Monte Carlo simulation, the time sequence of Monte Carlo events is constructed following a probability density function which is derived based on the same assumptions (Assumptions 1–3) as those used in the derivation of the master equation (Gillespie, 1976).

A Monte Carlo event is characterized by both the type of the event (adsorption or migration of Ga atoms in our application) and the site in which the event is executed. We use $e(x; i, j)$ to represent a Monte Carlo event of type x executed on the site (i, j), where $x \in \{a, m\}$, where $x = a$ corresponds

to an adsorption event and $x = m$ corresponds to a migration event, $1 \leq i, j \leq N$, and $N \times N$ is the size of the lattice.

The sequence of Monte Carlo events can be constructed based on the probability density function, $F(\tau, e)$, defined as follows.

Definition 1. $F(\tau, e)\,\mathrm{d}\tau$ is the probability at time t that event e will occur in the infinitesimal time interval $(t + \tau, t + \tau + \mathrm{d}\tau)$.

We now compute the expression of $F(\tau, e)$ based on Assumptions (1) and (2):

$$F(\tau, e)\,\mathrm{d}\tau = P_{0\tau} P_e \tag{7}$$

where $P_{0\tau}$ is the probability that no event occurs in $[t, t + \tau)$ and P_e is the probability that event e occurs in the time interval $(t + \tau, t + \tau + \mathrm{d}\tau)$. P_e can be determined by using Assumption 3 as follows:

$$P_e = W_e\,\mathrm{d}\tau \tag{8}$$

$P_{0\tau}$ can be calculated by sampling the duration $(t, t + \tau)$ into M identical time intervals $\delta\tau = \tau/M$. When $M \to \infty$, $\delta\tau$ is small enough so that each time interval of size $\delta\tau$ contains one event at most. Based on Assumption 3, the probability that one event e occurs in $\delta\tau$ is $W_e\delta\tau$ and based on Assumption 2, the probability that any one event occurs in $\delta\tau$ is $\sum_e W_e\delta\tau$. Therefore, the probability that no events will occur in $\delta\tau$ is

$$P_{0\delta\tau} = 1 - \sum_e W_e\delta\tau \tag{9}$$

where $P_{0\delta\tau}$ is the probability that no event occurs in one $\delta\tau$ interval and $W_e\delta\tau$ is the probability that one event e will occur in the $\delta\tau$ interval.

Eq. (9) can be applied to all the $\delta\tau$ time intervals in the duration $(t, t + \tau)$. Therefore, the probability that no events will occur in the duration τ is

$$P_{0\tau} = \lim_{N\to\infty} P_{0\delta\tau}^N = \lim_{N\to\infty} \left(1 - \frac{\sum_e W_e\tau}{N}\right)^N = \exp\left(-\sum_e W_e\tau\right) \tag{10}$$

By substituting Eqs. (8) and (10) into Eq. (7) and using $W_{\mathrm{tot}} = \sum_e W_e$, the probability density function, $F(\tau, e)$, is as follows:

$$F(\tau, e) = W_e\ \exp(-W_{\mathrm{tot}}\tau) \tag{11}$$

Monte Carlo simulation constructs the sequence of events following the probability density function shown in Eq. (11). Note that Eq. (11) is based on the same assumptions as the master equation (Eq. (6)), therefore, the Monte Carlo simulation is able to provide an unbiased realization of a stochastic process which is consistent with that described by the master equation. There are many Monte Carlo algorithms available to simulate a stochastic dynamic process. In this study, the kinetic Monte Carlo simulation algorithm developed by Vlachos (1997) (see also Lam & Vlachos, 2001) was used to simulate the surface roughness of the GaAs surface. This algorithm is a modification of the so-called "direct" method developed by Gillespie (1976). In the remainder of this section, we discuss in detail the theoretical foundation and steps of the "direct" method and of the algorithm used in the calculations. The "direct" method is based on the fact that the two-variable probability density function, Eq. (11), can be written as the product of two one-variable probability functions:

$$F(\tau, e)\,\mathrm{d}\tau = F_1(\tau)\,\mathrm{d}\tau \cdot P(e|\tau) \tag{12}$$

where $F(\tau, e)\,\mathrm{d}\tau$ is the probability that event e will occur in the time interval $(t + \tau, t + \tau + \mathrm{d}\tau)$, $F_1(\tau)\,\mathrm{d}\tau$ is the probability that an event will occur in the time interval $(t + \tau, t + \tau + \mathrm{d}\tau)$ and $P(e|\tau)$ is the probability that the next event will be event e, given that the next event will occur in $(t + \tau, t + \tau + \mathrm{d}\tau)$.

Based on the addition theorem (Melsa & Sage, 1973), $F_1(\tau)\,\mathrm{d}\tau$ is the sum of $F(\tau, e)\,\mathrm{d}\tau$ over all events:

$$F_1(\tau)\,\mathrm{d}\tau = \sum_e F(\tau, e)\,\mathrm{d}\tau \tag{13}$$

$P(e|\tau)$ can be obtained by substituting Eq. (13) into Eq. (12):

$$P(e|\tau) = \frac{F(\tau, e)}{\sum_e F(\tau, e)} \tag{14}$$

By substituting Eq. (11) into Eqs. (13) and (14), we obtain:

$$F_1(\tau) = W_{\mathrm{tot}}\ \exp\left(-W_{\mathrm{tot}}\tau\right) \tag{15}$$

$$P(e|\tau) = \frac{W_e}{W_{\mathrm{tot}}} \tag{16}$$

In the Monte Carlo simulation, Eq. (15) is used to determine the life time of a Monte Carlo event and Eq. (16) is used to determine the Monte Carlo event to be executed. To execute a Monte Carlo simulation, a pseudo-random number generator is used which generates random numbers following the uniform distribution in the interval (0, 1). It has been proven by Gillespie (1976) that if a random number, ξ, follows the uniform distribution in the unit interval, then the life time of a Monte Carlo event, τ, can be computed by

$$\tau = -\frac{\ln\,\xi}{W_{\mathrm{tot}}} \tag{17}$$

To demonstrate that the τ obtained by using Eq. (17) follows the probability density function in Eq. (15), we first compute the probability that $\tau < T$ ($P(\tau < T)$), using Eq. (17). Specifically, we have

$$P(\tau < T) = P\left(-\frac{\ln\,\xi}{W_{\mathrm{tot}}} < T\right) = P(\exp(-W_{\mathrm{tot}}T) < \xi < 1) \tag{18}$$

Because ξ follows the uniform distribution in the interval (0, 1), from Eq. (18) we have that

$$P(\tau < T) = P(\exp(-W_{\text{tot}}T) < \xi < 1) = 1 - \exp(-W_{\text{tot}}T) \tag{19}$$

whose corresponding probability density function, $F_1'(\tau)$, is

$$F_1'(\tau) = \frac{\mathrm{d}P(\tau < T)}{\mathrm{d}T} = W_{\text{tot}} \exp(-W_{\text{tot}}T) \tag{20}$$

which is the probability density function in Eq. (15). Therefore, the life time of each Monte Carlo event, τ, calculated using Eq. (17) follows the probability density function in Eq. (15), which is consistent to the master equation.

The Monte Carlo algorithm picks an event to be executed based on the probability of Eq. (16). In this study, we assume that the probability of adsorption in an infinitesimal time interval $\delta\tau$ is site-independent and the probability of migration is only dependent on the number of immediate side neighbors. Therefore, the following algorithm presented in Lam and Vlachos (2001) is used to pick a Monte Carlo event, which is consistent with Eq. (16). First, the surface atoms are grouped into five classes based on the number of side neighbors (e.g., surface atoms have 0, 1, 2, 3 and 4 side neighbors), in each class, the atoms have the same migration probabilities (adsorption probability is site-independent). The total rate of adsorption, W_{a} is computed as follows:

$$W_{\text{a}} = N^2 w_{\text{a}} \tag{21}$$

where N is the size of the lattice and w_{a} is the adsorption rate of Ga atoms on each surface site.

The total rate of migration, W_{m} is given by:

$$W_{\text{m}} = \sum_{i=0}^{4} W_{\text{m}_i} \tag{22}$$

$$W_{\text{m}_i} = M_i \nu_0 \exp\left(-\frac{E_{\text{s}} + iE_{\text{n}}}{k_{\text{B}}T}\right) \tag{23}$$

where M_i is the number of surface Ga atoms that have i side neighbors and the value of M_i is equal to the number of atoms in each of the five classes.

Then a random number following the uniform distribution in the unit interval, ζ, is generated to select an event based on the rates. Specifically, if $0 < \zeta < W_{\text{a}}/(W_{\text{a}} + W_{\text{m}})$, the event is adsorption; if $W_{\text{a}}/(W_{\text{a}} + W_{\text{m}}) < \zeta < 1$, the event is migration. If the event is migration, the kth class in which the migration event will occur is selected by finding out an integer, $k \in \{0, 1, 2, 3, 4\}$ such that $(W_{\text{a}} + \sum_{i=0}^{k-1} W_{\text{m}_i})/(W_{\text{a}} + W_{\text{m}}) < \zeta < (W_{\text{a}} + \sum_{i=0}^{k} W_{\text{m}_i})/(W_{\text{a}} + W_{\text{m}})$. After that, a second random number is generated to select the site where the event will be executed; if the event is adsorption, the site is randomly picked from sites in the entire lattice; if the event is migration, the site is randomly picked from the list of the sites in the selected class.

After the site is selected, the MC event is executed. If the event is adsorption, it is executed by adding one atom on the selected site; if the event is migration, a third random number is generated to randomly pick a neighboring site that has a lower height (target site), and move the atom from the original site to the target site. After an MC event is executed, the five classes are updated and the next step of the simulation can be performed. Upon an executed event, a real-time increment Δt is computed by applying Eq. (17) to our process:

$$\Delta t = \frac{-\ln \xi}{W_{\text{a}} + W_{\text{m}}} \tag{24}$$

where ξ is a random number in the (0, 1) interval. This algorithm guarantees that every trial is successful and is efficient compared to traditional null event algorithms (Reese, Raimondeau, & Vlachos, 2001).

3. Computation of kinetic Monte Carlo model parameters using experimental data

The predictions of the Monte Carlo simulation depend on the rates of adsorption and migration used in the calculations. When the film growth rate is fixed (which is the case in our process), the rate of adsorption can be directly calculated based on the growth rate. However, there are three parameters in the expression for the migration rate, ν_0, E_{s} and E_{n}, in Eq. (2) that need to be determined. In this study, the values for these parameters are calculated using experimental data. In the case of GaAs thin-film growth by MBE, values for the E_{s} and E_{n} have been obtained from the measurements of reflection high-energy electron diffraction (RHEED) specular intensities so that the transition temperature predicted by the MC simulation matches that of the measured data (Shitara et al., 1992b). Furthermore, we adjust the values for the three parameters in Eq. (2) so that the dependence of surface roughness on the substrate temperature measured in the experimental work of Law et al. (2000) can be predicted by the MC simulations.

To compare the roughness from MC simulations to experimental values reported in Law et al. (2000), we first give a description of the definition of surface roughness used in that paper. Surface roughness is a measure of fluctuation of surface height and can be defined as (Sinha, Sirota, Garoff, & Stanley, 1988; Tanenbaum, Laracuente, & Gallagher, 1997):

$$r'(L) = \sqrt{G(L)}, \quad G(L) = \langle [h(x_i, y_i) - h(x_j, y_j)]^2 \rangle \tag{25}$$

where $G(L)$ is the height–height correlation function, $h(x_i, y_i)$ and $h(x_j, y_j)$ are the surface heights at locations i and j separated by a lateral distance, L, and $r'(L)$ is the roughness. The notation $\langle \cdot \rangle$ denotes an ensemble average over all possible pairs of surface points.

Table 1
Parameters for migration rate in GaAs thin-film growth by MBE (Shitara et al., 1992b)

E_s (eV)	1.58
E_n (eV)	0.28
k_B (J/K)	1.38×10^{-23}
h (J s)	6.63×10^{-34}

The surface roughness defined in this way follows a power-law dependence on the lateral separation up to a certain value denoted as the critical length, L_c, and saturates when the lateral separation is larger than the critical length (Sinha et al., 1988; Palasantzas, 1993). This leads to the following expressions for surface roughness:

$$r'(L) = \begin{cases} kL^{\alpha} & \text{for } L < L_c, \\ r'(\infty) & \text{for } L > L_c \end{cases} \tag{26}$$

where α is the roughness exponent, k is a constant and $r'(\infty)$ is the saturated roughness value.

The values for $r'(\infty)$, α and L_c were measured in Law et al. (2000). In our simulation, a power-law dependence of surface roughness on the lateral separation up to a certain critical length is also observed. The value for the saturated roughness from our MC simulations is tuned to fit the experimental data reported in Law et al. (2000)by adjusting the parameters of the migration rate. Note that the MC simulation cannot predict the values for critical length and roughness exponent reported in the experimental data.

To determine the parameters for migration rate to match the experimental results, we use the parameters reported in Shitara et al. (1992b) for GaAs thin-film growth by MBE as our initial estimate for the parameters of Eq. (2) and run kinetic MC simulations for the evolution of surface roughness of GaAs (0 0 1) surface. The parameters used as initial estimates are listed in Table 1, where k_B is the Boltzmann's constant, h is the Planck's constant and $\nu_0 = 2k_BT/h$, where T is the substrate temperature. We employ a cubic lattice in all kinetic MC simulations. Note that the crystal structure of GaAs is a Zinc–Blend-type structure, but the (0 0 1) surface of Zinc–Blend structure is identical to a cubic lattice except from the fact that there is a shift of a half unit of the lattice at each atomic layer in the Zinc–Blend structure (Blakemore, 1982). This shift is not considered in this study. The thickness of one layer of GaAs is 2.8 Å and the lattice constant of the cubic lattice used in our simulations is 3.99 Å. The growth rate is 0.5 μm/h, which corresponds to $w_a = 0.49\,s^{-1}$. MC simulations are performed on an 80×80 lattice at four different substrate temperatures ($T = 713, 750, 775$ and 800 K). Note, in the experimental work of Law et al. (2000), the GaAs thin-film surface roughness is measured by STM after cooling down the film to room temperature therefore, the cooling down process is also simulated. During the cooling down process, there is no supply of precursors, but the surface migration still takes place. Therefore, during the cooling process, we set the adsorption rate, $w_a = 0$ and use the same migration rate (Eq. (2)) in all the simulations. The film is cooled down at

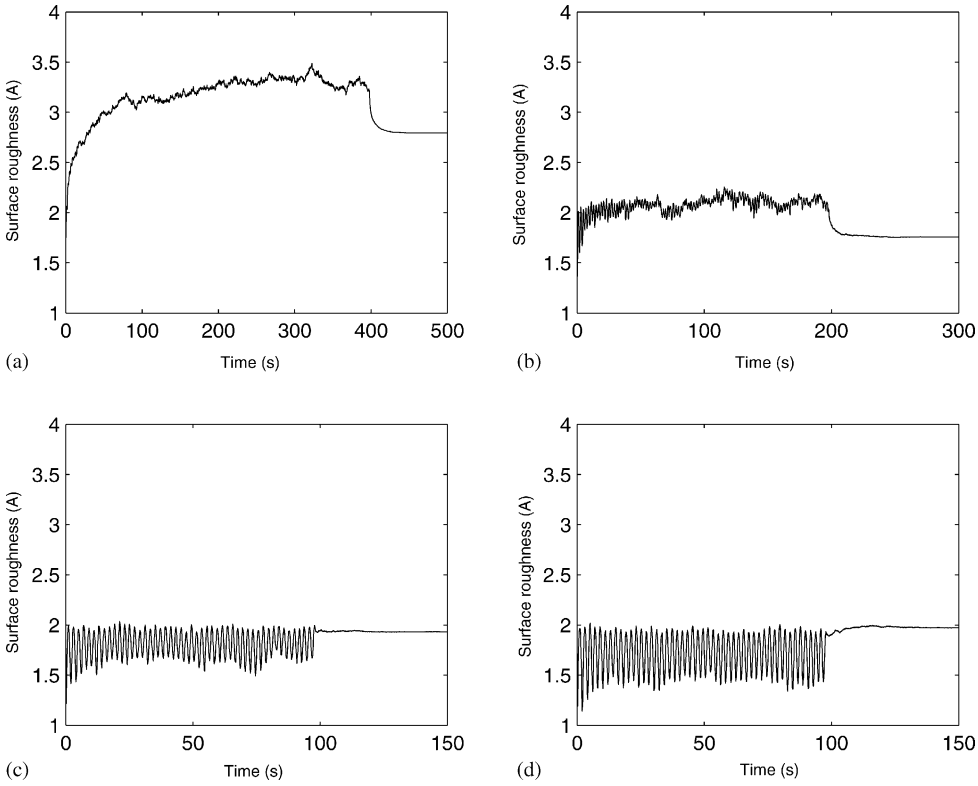

Fig. 1. Surface roughness under different substrate temperatures when the parameters of migration rate are the same to those for GaAs thin-film growth by MBE reported in Shitara et al. (1992b): (a) $T = 713$ K, (b) $T = 750$ K, (c) $T = 775$ K and (d) $T = 800$ K.

a rate of 2 K/s, which is reported in Law et al. (2000). Fig. 1(a) shows the evolution of surface roughness when $T = 713$ K. During growth, the surface roughness is ∼3.3 Å. The growth stops at $t = 400$ s and the surface roughness declines to 3.0 Å after the cooling down process. Fig. 1(b) show the evolution of surface roughness when $T = 750$ K. During growth, the surface roughness is ∼2.3 Å. The growth stops at $t = 200$ s and the surface roughness declines to ∼1.7 Å after the cooling down process. Fig. 1(c) and (d) show the evolution of surface roughness when $T = 775$ and 800 K. During growth, the surface roughness fluctuates between 1.5 and 2.0 Å. The growth stops at $t = 100$ s and the surface roughness stays at ∼2.0 Å after the cooling down process. The experimental results of saturated surface roughness after the growth of a 0.5 μm thick GaAs film are Law et al. (2000): $r'(\infty) = 2.8$ Å when $T = 825$ K and $r'(\infty) \approx 1.3$ Å when $T = 850, 875$ and 900 K.

Comparing the simulation results for saturated surface roughness to the experimental data, we find that the saturated roughness obtained from MC simulation when $T = 713$ K is very close to the experimental data for saturated surface roughness when $T = 825$ K, and the saturated roughness obtained from MC simulation when $T = 775$ and $T = 800$ K is very close to the experimental data for saturated surface roughness when $T = 900$ K. Therefore, we compute the parameters for the migration rate in GaAs thin-film growth by MOCVD using the following method.

Let ν_0', E_s' and E_n' be the parameters of the migration rate in GaAs thin-film growth by MOCVD. We compute ν_0' and E_s' by constructing two equations for ν_0' and E_s'. To construct these two equations, we set the migration rate of adatoms (surface atoms without side-neighbor) in MOCVD, when substrate temperature is $T = 825$ K, equal to the migration rate of adatoms in MBE when substrate temperature is $T = 713$ K. Also, we set the migration rate of adatoms in MOCVD, when substrate temperature is $T = 900$ K, equal to the migration rate of adatoms in MBE when substrate temperature is $T = 788$ K ($T = 788$ K is the average of $T = 775$ and $T = 800$ K). This averaged temperature is used because the experimental data for saturated roughness when $T = 900$ K in MOCVD is very close to the saturated roughness obtained from MC simulations under both $T = 775$ and $T = 800$ K (when the parameters in Table 1 are used). Therefore, we have the following equations for ν_0' and E_s':

$$\nu_0' \exp\left(-\frac{E_s'}{k_B T_1'}\right) = \frac{2k_B T_1}{h} \exp\left(-\frac{E_s}{k_B T_1}\right) \tag{27}$$

$$\nu_0' \exp\left(-\frac{E_s'}{k_B T_2'}\right) = \frac{2k_B T_1}{h} \exp\left(-\frac{E_s}{k_B T_2}\right) \tag{28}$$

where the values of E_s, k_B and h are listed in Table 1, and $T_1 = 713$ K, $T_2 = 788$ K, $T_1' = 825$ K and $T_2' = 900$ K.

By solving Eqs. (27) and (28), $E_s' = 1.83$ eV and $\nu_0' = 2.9 \times 10^{13}\,s^{-1}$. Finally, the value of E_n' can be computed by setting the migration rate of surface atoms with 1 side-neighbor in MOCVD, when the substrate temperature is $T = 825$ K, equal to the migration rate of surface atoms with 1 side-neighbor in MBE when the substrate temperature is $T = 713$ K, resulting in the following equation for E_n':

$$\nu_0' \exp\left(-\frac{E_s' + E_n'}{k_B T_1'}\right) = \frac{2k_B T_1}{h} \exp\left(-\frac{E_s + E_n}{k_B T_1}\right) \tag{29}$$

where the values of E_s, k_B and h are listed in Table 1, $\nu_0' = 2.9 \times 10^{13} s^{-1}$, $E_s' = 1.83$ eV, $T_1 = 713$ K, and $T_1' = 825$ K.

By solving Eq. (29), $E_n' = 0.27\,\text{eV} = 0.15E_s'$, and this relationship is similar to the one reported in Shitara et al. (1992b) (specifically, $E_n = 0.15E_s$) in GaAs thin-film growth by MBE. The value of E_s' obtained following this method is also reasonably close to the value of E_s in MBE (Shitara et al., 1992b) and to those reported for MOCVD of GaAs thin films (Law et al., 2000). Furthermore, by comparing the simulation results for the saturated roughness for $T = 850$ K and $T = 875$ K to experimental data, and increasing the pre-exponential factor, ν_0' from $2.9 \times 10^{13}\,s^{-1}$ to $5.8 \times 10^{13}\,s^{-1}$ a better match of all the simulation results, for $T = 825, 850, 875$ and 900 K, to the experimental data in Law et al. (2000) can be achieved.

Table 2
Parameters for migration rate obtained by fitting kinetic Monte Carlo simulation results to the experimental results reported in Law et al. (2000)

ν_0 (s^{-1})	5.8×10^{13}
E_s (eV)	1.82
E_n (eV)	0.27

The values of the migration rate parameters, obtained by following the above method and used in all the simulations are given in Table 2. Fig. 2(a) and (b) show the evolution of surface roughness after 400 s of deposition time when the substrate temperatures are $T = 825$ K and 850 K, respectively. Fig. 2(c) and (d) show the evolution of surface roughness after 100 s of deposition time when the substrate temperatures are 875 and 900 K, respectively. The saturated roughness from all the simulations are very close to the experimental data reported in Law et al. (2000).

Remark 1. Note that the critical length and the roughness exponent measured in Law et al. (2000) cannot be obtained from our kinetic MC simulation by adjusting the simulation parameters. We believe that the critical length and roughness exponent are related to the actual island size on the surface. In the simulation, the sizes of surface islands have to be smaller than the size of the simulation lattice. Limited by the available computing power, the size of simulation lattice is not comparable to the size of the wafer, so the actual island size cannot be adequately captured within the small simulation lattice (320 Å × 320 Å) used in the present study. However, the saturated surface roughness, $r'(\infty)$, can be considered as a measure of the fluctuation of height of the surface because it is independent of the influence of the size of surface islands (the lateral separation is much larger than the sizes of surface islands and each surface pair picked in the height–height cor-

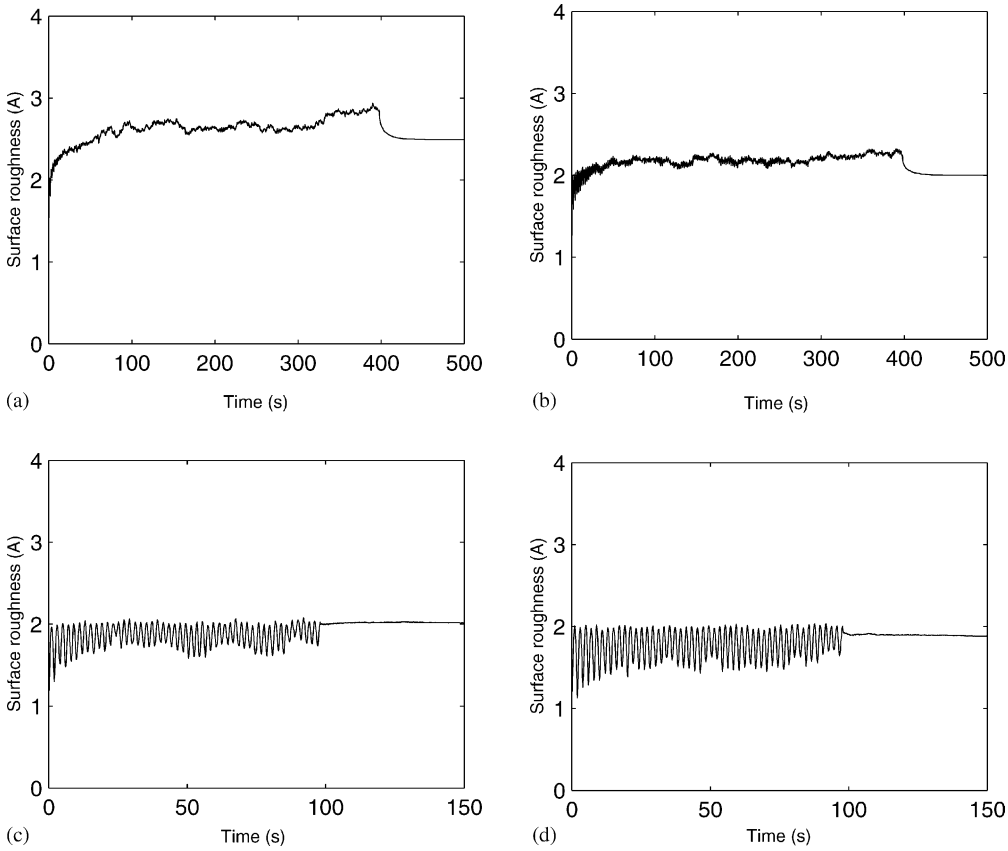

Fig. 2. Surface roughness under different substrate temperatures when the parameters of migration rate are adjusted to match the experimental results reported in Law et al. (2000): (a) $T = 825$ K, (b) $T = 850$ K, (c) $T = 875$ K and (d) $T = 900$ K.

relation are on different islands on the surface). We use the roughness defined in Eq. (26) because this is the roughness used in Law et al. (2000) to compare and fit the simulation results to experimental data.

Remark 2. Note that in experimental studies, the surface roughness of GaAs thin films was measured after a deposition of 0.5μm thick film, which corresponds to a deposition time of about 1 h. Owing to computational limitations, the simulated deposition time is much shorter that 1 h. However, from the simulation results presented in Figs. 1 and 2, it can be seen that after an initial transient of $\sim$100 s, the roughness either converges to some fixed value (see plots (a) and (b) of Figs. 1 and 2) or oscillates around some fixed value (see plots (c) and (d) of Figs. 1 and 2). Therefore, it can be concluded that further increase in the simulation time will lead to the same surface roughness for the GaAs thin film.

Remark 3. Note that in Shitara et al. (1992b), the pre-exponential factor, ν_0, has a linear dependence on substrate temperature ($\nu_0 = 2k_B T/h$). However, this is a weak temperature dependence compare to the Arrhenius-like dependence of the migration rate of the substrate temperature. Therefore, we assume that the pre-exponential factor in Eq. (2) is a constant. The same assumption can also be found in other Monte Carlo simulation studies of GaAs thin-film growth reported in the literature (see, e.g., Heyn, Franke, & Anton, 1999; Meng & Weinberg, 1996). Furthermore, the simulation results show that by assuming that the pre-exponential factor in Eq. (2) is a constant, the saturated roughness predicted by kinetic MC simulations under different substrate temperatures is very close to the experimental data.

4. Real-time estimation of thin-film surface roughness

Surface roughness is the property of interest from a control point of view since it directly influences device properties. To be able to achieve real-time control of surface roughness of GaAs thin films, it is important to develop an estimator that can provide estimates of surface roughness in real-time. In this section, we develop such an estimator by following a methodology that was recently proposed in Lou and Christofides (2003a).

For consistency with the previous work, the roughness, r, is represented by the standard deviation of the surface from its average height and is computed as follows:

$$r = \sqrt{\frac{\sum_{i=1}^{N}\sum_{j=1}^{N}[h_{i,j} - h]^2}{N \times N}} \tag{30}$$

where N is the size of the lattice, h is the average height of the surface and $h_{i,j}$ is the height of the surface at site (i, j); note that estimation and control of surface roughness using alternative surface roughness definitions can be readily studied within this framework.

In the kinetic MC simulation, the size of the lattice influences the quality of the predictions and the computational demand. In a previous work, Lou and Christofides (2003a) discussed the dependence of simulation results on the lattice size used in the MC simulations. The simulation results show that when the lattice size is sufficiently large, the roughness profiles obtained from kinetic MC simulations are independent of the lattice size. To implement real-time feedback control based on a model that captures the evolution of surface roughness, a small lattice must be used in the simulation to make the model solution time comparable to the process real-time. However, the roughness profiles from a kinetic MC simulation using a small lattice contain significant stochastic fluctuations, and thus, they cannot be directly used for feedback control (Lou & Christofides, 2003a,b); such an approach would result in significant fluctuations in the control action which could perturb unmodeled (fast) process dynamics and should be avoided.

Because each kinetic MC simulation run provides one realization of a stochastic process, by averaging the simulation results from different runs, the roughness obtained by averaging multiple kinetic MC simulations is closer to the expected roughness value obtained from the solution of the master equation, when compared to the roughness profile obtained from a single simulation run with a same size lattice. This result points to reducing the fluctuations on the surface roughness obtained from the kinetic MC simulation by independently running several small-lattice kinetic MC simulations with the same parameters and averaging the outputs of the different runs. In the simulations, when the surface roughness profiles are computed by averaging six independent runs of kinetic MC simulations which use a 30×30 lattice, the solution time of the kinetic MC model is comparable to the real-time process evolution and the average values of the surface roughness approximate well their expected values computed from the solution of the master equation, which are obtained by running the kinetic MC simulation on a 150×150 lattice. This is a sufficiently large lattice to ensure simulation results which are independent of the lattice size.

The predicted profile of surface roughness, which is obtained from a kinetic MC simulation based on multiple small-lattice models, still contains stochastic fluctuations and is not robust (due to the open-loop nature of the calculation) with respect to disturbances and variations in process parameters. To mitigate these problems, the approach proposed by Lou and Christofides (2003a) that combined the kinetic MC simulator, based on multiple small-lattice models, with an adaptive filter, to reject the stochastic fluctuations on the surface roughness profile, and a measurement error compensator to improve the estimates of surface roughness using on-line measurements was followed. Specifically, the adaptive filter is a second-order dynamical system with the following state-space representation:

$$\frac{\mathrm{d}\hat{y}_r}{\mathrm{d}\tau} = y_1, \qquad \frac{\mathrm{d}y_1}{\mathrm{d}\tau} = \frac{K}{\tau_\mathrm{I}}(y_r - \hat{y}_r) - \frac{1}{\tau_\mathrm{I}} y_1 \tag{31}$$

where y_r is the output of the kinetic MC simulation based on multiple small-lattice models, $\hat{y}_r$ is the filter output, K is the filter gain and τ_I is the filter time constant. To accelerate the response of the filter and avoid a large overshoot, $\tau_\mathrm{I} = 0.5/\mathrm{K}$. To achieve both fast tracking of the dynamics of the outputs and efficient noise rejection, the gain of the filter is adaptively adjusted as follows:

$$K(\tau) = K_0 \frac{|\int_{\tau-\Delta\tau}^{\tau} y_r(t)\,\mathrm{d}t - \int_{\tau-2\Delta\tau}^{\tau-\Delta\tau} y_r(t)\,\mathrm{d}t|}{\Delta\tau^2} + K_\mathrm{s} \tag{32}$$

where K_0 is a constant, K_s is the steady-state gain for the adaptive filter and $\Delta\tau$ is the time interval between two updates of K. Although a better tracking performance is expected when a small $\Delta\tau$ is used, a very small $\Delta\tau$ will not significantly reduce the effect of fluctuations on the filter output and should be avoided.

The measurement error compensator uses the available on-line measurements (in the numerical simulations the values of the surface roughness are obtained from the large lattice kinetic Monte Carlo simulator) to produce improved estimates of the surface roughness. The state-space representation of the measurement error compensator is

$$\frac{\mathrm{d}e}{\mathrm{d}\tau} = K_\mathrm{e}(y_h(\tau_{\mathrm{m}_i}) - \hat{y}(\tau_{\mathrm{m}_i})),$$
$$\tau_{\mathrm{m}_i} < \tau \le \tau_{\mathrm{m}_{i+1}},\ i = 1, 2, \ldots \tag{33}$$

and the final roughness estimates are computed using Eq. (34):

$$\hat{y} = \hat{y}_r + e \tag{34}$$

In the above equations, K_e is the compensator gain, e is the estimated model error, which is used to compensate the model output, $\hat{y}$ is the roughness estimates, $\hat{y}_r$ is the filtered output from a kinetic MC simulator which uses multiple small-lattice models and y_h is the output of a kinetic MC simulator which uses a large lattice. In an experimental set-up, y_h could be obtained from the measurement sensor. Since the roughness measurements are only available at discrete points in time $\tau_m = [\tau_{m_1}, \tau_{m_2}, \ldots]$, the right-hand side of Eq. (33) is computed at the time a roughness measurement is available and is kept at this value for the time interval between two available roughness measurements.

The combination of the adaptive filter and the measurement error compensator functions as an estimator, which is capable of accurately predicting the evolution of surface roughness during the thin-film growth. Fig. 3 shows the surface roughness profile computed by the estimator, which uses a kinetic MC simulator based on six 30×30 lattice models

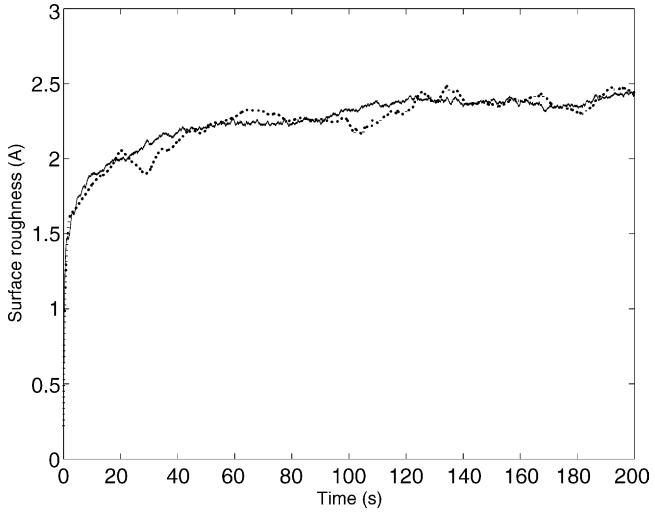

Fig. 3. Surface roughness profiles from the estimator (dotted line) and from a kinetic MC simulation which uses a 150 × 150 lattice model (solid line).

(solid lines). This profile is compared to the surface roughness profile obtained from a kinetic MC simulator which uses a150 × 150 lattice model. This comparison clearly shows that the developed estimator can accurately predict the evolution of surface roughness. Note that the developed estimator can be used for real-time feedback control, since the computational time needed to run kinetic MC simulation based on six 30 × 30 lattice models is comparable to the real-time process dynamics.

Remark 4. Referring to the selection of the lattice size, it is important to point out that while kinetic MC simulations based on multiple 30 × 30 lattice models can adequately capture the evolution of surface roughness in the specific thin-film growth problem under consideration, the dimension of the small lattice in general should be chosen so that the interactions between the surface atoms are adequately captured, and also that it is large enough to describe all the spatio-temporal phenomena occurring on the surface (e.g., cluster formation). Furthermore, the small lattice should be chosen to provide accurate estimates of the desired controlled properties. For example, in the case of surface roughness, this quantity is defined as the standard deviation of the surface from its average height. When a 30 × 30 small lattice is used, the computation of surface roughness involves hundreds of surface atoms, which is adequate to obtain the expected value. However, when the property of interest is, e.g., step density, a larger lattice is needed to obtain a convergent average value from the kinetic MC simulation. At this point, it is important to note that the proposed reduction of lattice size can be viewed as an alternative way to perform order reduction of the master equation (see Gallivan & Murray, 2003 for reduction approaches based directly on the master equation). Finally, note that through extensive simulations for our process, a 150 × 150 lattice is of sufficient size to capture the evolution of the film growth and that further increase of the lattice size leads to no observable improvement in the accuracy of the simulation results. Therefore, in the remainder of this study, a kinetic MC simulator which uses a 150 × 150 lattice to describe the evolution of the thin-film growth in the closed-loop system is used.

5. Feedback control of surface roughness

The production of high-quality thin films requires that the surface roughness is maintained at a desired level. In this study, we consider feedback control of surface roughness of GaAs thin films by manipulating the substrate temperature, which is assumed to change only with respect to time. This is a reasonable formulation for the manipulated input and is practically feasible for many experimental and industrial deposition processes. With such a manipulated input formulation, however, it is only possible to achieve control of a spatially averaged surface roughness, e.g., the one defined in Eq. (30). We could have formulated a control problem under the assumption that a large number of manipulated inputs (control actuators) are available to control surface roughness with higher precision but such a control problem formulation would not be practically feasible at the present time. As will be shown, it is possible by manipulating the substrate temperature (single input formulation) to achieve an overall very smooth film surface configuration.

The fact that the model that describes the evolution of the thin-film growth process is not available in closed-form (available only as a kinetic MC model) motivates the use of a proportional–integral (PI) feedback controller to regulate the surface roughness. Furthermore, from simulation results shown in Fig. 2, even when the substrate temperature is fixed, the surface roughness oscillates around a fixed value. This oscillatory behavior is an intrinsic characteristic of the film growth process and is not the control objective to eliminate this oscillation, rather to control the surface roughness at a desired level (range). To eliminate unnecessary control actions, which may lead to poor closed-loop performance, the control objective is to stabilize the surface roughness value close to a desired level within certain tolerance ϵ. For this purpose, a proportional–integral (PI) feedback control algorithm is used of the following form:

$$u(\tau) = K_c \left[\hat{e} + \frac{1}{\tau_c} \int_0^\tau \hat{e}(t)\, dt \right] \tag{35}$$

$$\hat{e}(t) = \begin{cases} \hat{y} - y_{set} & \text{for } |\hat{y} - y_{set}| > \epsilon, \\ 0 & \text{for } |\hat{y} - y_{set}| \leq \epsilon \end{cases} \tag{36}$$

where y_{set} is the desired level of surface roughness, $\hat{y}$ is the output of the roughness estimator, K_c is the proportional gain and τ_c is the integral time constant.

The PI controller is coupled with the roughness estimator as shown in Fig. 4. The roughness estimator includes a kinetic

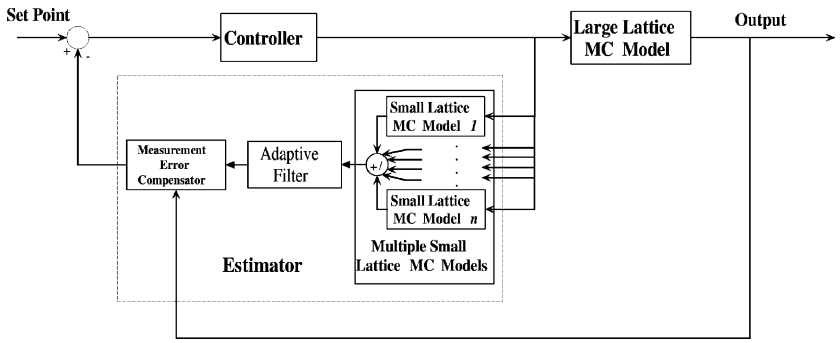

Fig. 4. Diagram of the closed-loop system under the developed estimator/controller structure.

MC simulator which uses multiple small-lattice models, the adaptive filter and the measurement error compensator. The output of the kinetic MC simulator is sent to the adaptive filter (Eq. (31)) to suppress the noise, and then, the measurement error compensator (Eqs. (33) and (34)) further corrects the filtered roughness based on the measurements and the roughness estimates are used in the PI controller to determine the substrate temperature. Several closed-loop simulation runs were performed to evaluate the effectiveness of the developed estimator/controller structure shown in Fig. 4. In these simulations, the outputs from six kinetic MC simulators using 30×30 lattice models are averaged within the estimator. A 150×150 lattice MC model is used to describe the evolution of the process, which corresponds to a 600 Å $\times$ 600 Å GaAs (0 0 1) surface. The desired roughness is 1.5 Å and the tolerance is 0.1 Å. The time interval between two available measurements is taken to be 3.0 s. This specification is made based on the fact that high-speed scanning tunnelling microscopy (STM) (Curtis, Mitsui, & Ganz, 1997) is able to measure the morphology of a 600 Å $\times$ 600 Å surface with an acquisition time of 3 s and the fact that it is feasible to perform STM measurement during epitaxial growth of GaAs layers (Voigtländer, 2001). The parameters for the roughness estimator and the PI controller used in the simulations are given in Table 3. Initially, the GaAs thin film grows on a perfect surface at $T = 800$ K with the roughness increasing. The controller is activated when the roughness reaches 2.3 Å. Fig. 5 shows the evolution of surface roughness under feedback control. Fig. 6 shows the profile of the substrate temperature. The results clearly show that the developed estimator/controller structure can successfully drive the surface roughness to the desired level. To test the robustness of the proposed estimator/controller structure, the GaAs thin-film

Table 3
Roughness estimator and controller parameters

K_0 (s/Å)	0.05
K_s	0.1
K_e (s^{-1})	0.08
K_c (K/Å)	15
τ_c (s)	0.2
ϵ (Å)	0.1

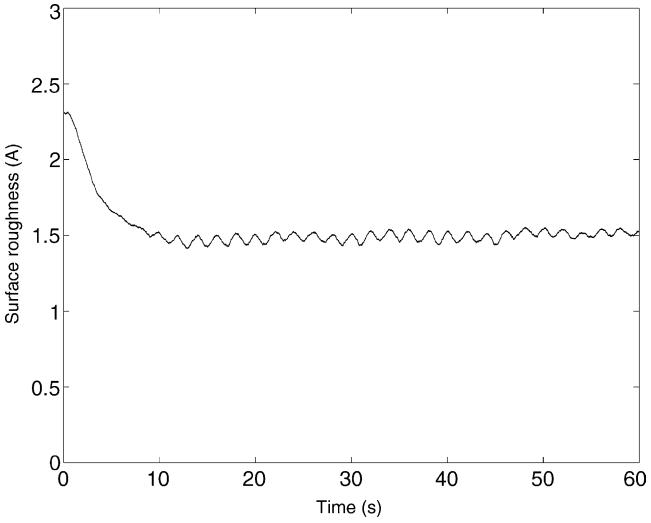

Fig. 5. Evolution of the surface roughness under feedback control based on the roughness estimator.

growth process is assumed to have a 10% uncertainty in the energy associated with a single bond on the surface, i.e., the E_s used in the roughness estimator is 1.82 eV but the E_s used in the kinetic MC model based on the large lattice is 2.0 eV.

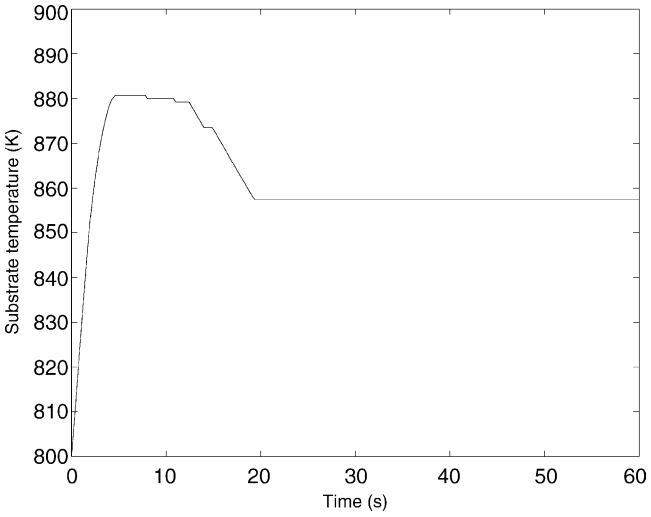

Fig. 6. Evolution of the substrate temperature under feedback control based on the roughness estimator.

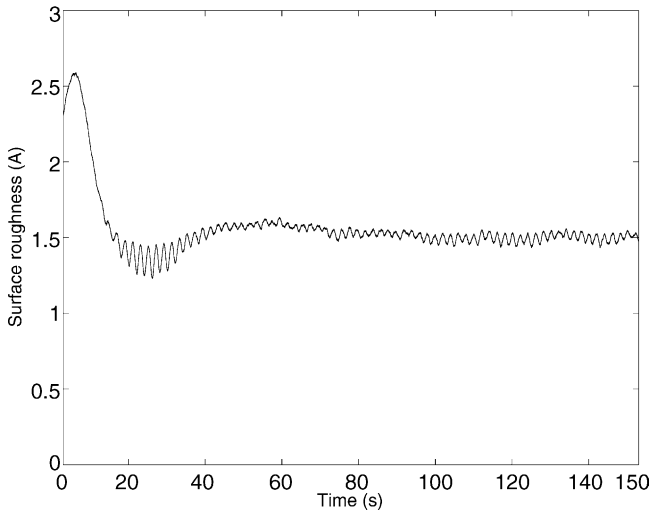

Fig. 7. Evolution of the surface roughness under feedback control based on the roughness estimator; closed loop system simulation under uncertainty.

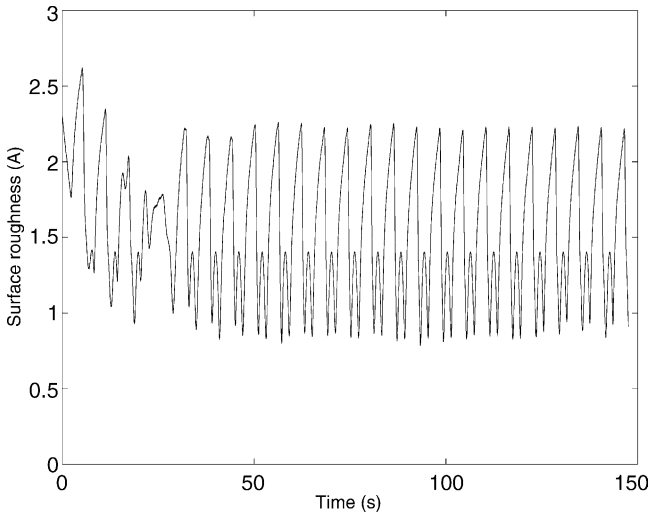

Fig. 9. Evolution of the surface roughness under feedback control without roughness estimator.

Figs. 7 and 8 show the corresponding output and input profiles, respectively. Note that the controller does exhibit very good robustness behavior (compare also Figs. 5 and 7). To show the importance of using the roughness estimator for feedback control and not relying exclusively on the roughness measurements (which are obtained only every 3.0 s), the PI controller (parameters as Table 3) is applied to the kinetic MC model assuming that new roughness measurements are fed to the controller every 3.0 s, which is consistent with the previous simulations. Also, to prevent the substrate temperature from obtaining unreasonably high or low values, the substrate temperature is constrained to be $750\,\mathrm{K} \leq T \leq 950\,\mathrm{K}$. Note that when the roughness is controlled using the proposed controller/estimator structure, the substrate temperature is always within $750\,\mathrm{K} \leq T \leq 950\,\mathrm{K}$ (see Fig. 6). Figs. 9 and 10 show the evolution of surface roughness and substrate temperature, respectively. We can see that the PI controller, based on discrete roughness measurements, is not able to control the surface roughness to the desired level which demonstrates the usefulness of the proposed estimator/controller structure.

Remark 5. Note that by tuning the PI controller, the surface roughness could be controlled to the desired level by using only the on-line roughness measurements. However, further controller tuning cannot achieve a closed-loop performance as good as that achieved under feedback control using the roughness estimator. To show this, we applied the PI controller with a new set of parameters ($K_c = 5\,\mathrm{K/Å}$, $\tau_c = 1.0\,\mathrm{s}$) to the same kinetic MC model for the GaAs thin-film growth process, assuming that new roughness measurements are fed into the controller every 3.0 s. The parameters of the PI controller are tuned to make the controller drive the surface roughness to the desired level. Figs. 11 and 12 show the profiles of surface roughness and substrate temperature, respectively. With the new controller parameters, the surface

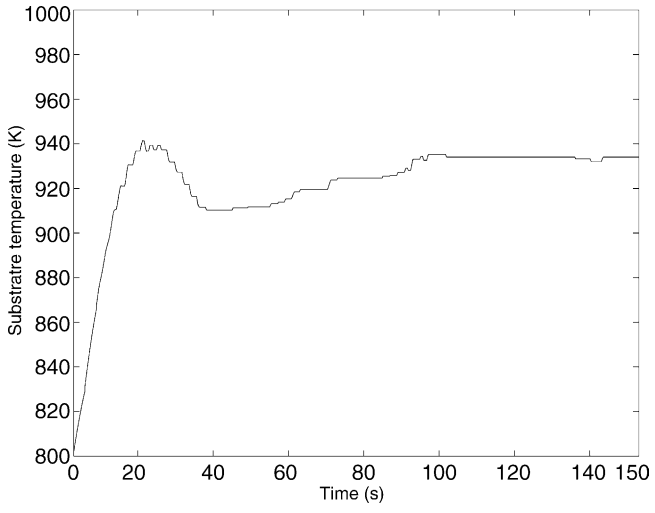

Fig. 8. Evolution of the substrate temperature under feedback control based on the roughness estimator; closed loop system simulation under uncertainty.

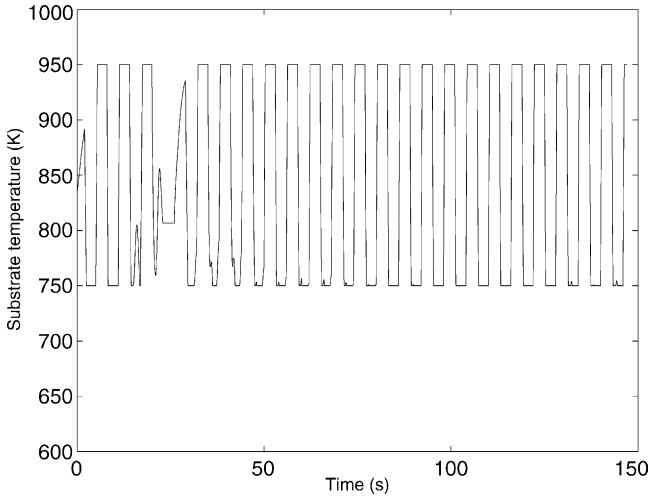

Fig. 10. Evolution of the substrate temperature under feedback control without roughness estimator.

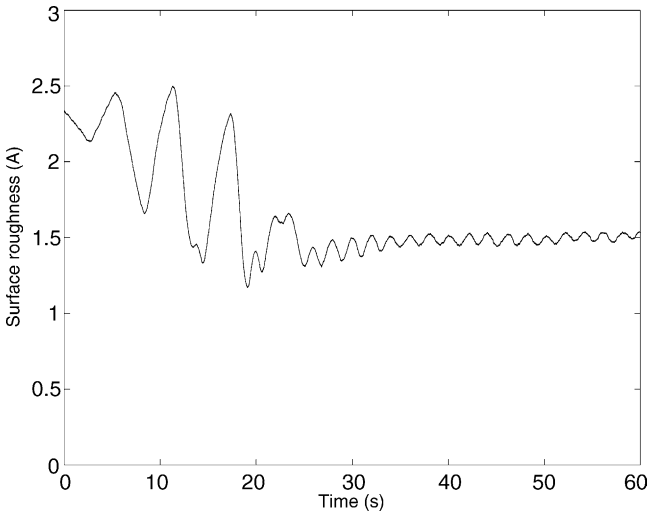

Fig. 11. Evolution of the surface roughness under feedback control without roughness estimator.

roughness is eventually controlled to the desired level, but significant oscillations can be observed in the closed-loop roughness profile and the process takes significantly longer time to reach the desired level (compare Figs. 5 and 11; in Fig. 5, the surface roughness in the closed-loop simulation reaches the desired level at about $t = 10$ s, but in Fig. 11, the surface roughness in the closed-loop simulation reaches the desired level at about $t = 30$ s). To better compare the closed-loop performance using different tuning parameters, the closed-loop roughness profiles shown in Figs. 5 and 11 are shown together in Fig. 13. Also, many other sets of tuning parameters for the PI controller were tested; the conclusion is that it is difficult to simultaneously achieve short transient time and reduced oscillation when control of the surface roughness is performed using discrete roughness measurements.

Remark 6. The effect of time delays in the measurements of surface roughness on the closed-loop system performance

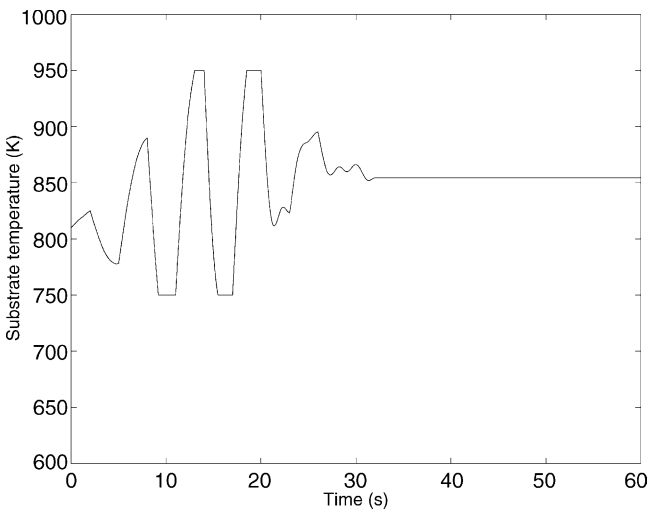

Fig. 12. Evolution of the substrate temperature under feedback control without roughness estimator.

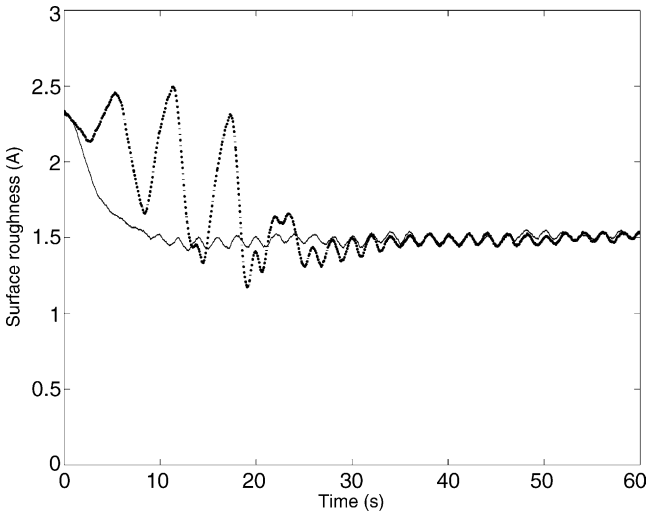

Fig. 13. Comparison of roughness profiles: (1) roughness profile under feedback control based on the roughness estimator (solid line) and (2) roughness profile under feedback control without roughness estimator with controller parameters $K_c = 5\,\text{K/Å}$, $\tau_c = 1.0$ s.

under the developed estimator/controller structure was also evaluated. To this end, we applied the estimator/controller structure (the parameters of the roughness estimator and the PI controller are shown in Table 3) to the process model based on a 150 × 150-lattice kinetic Monte Carlo simulator assuming that the new roughness measurements are available every 3.0 s but with a time-delay of $t_d = 3.0$ s. The resulting profiles of surface roughness and substrate temperature are shown in Figs. 14 and 15. The developed estimator/controller structure successfully drives the surface roughness to the desired level in the presence of a large time-delay in the roughness measurements.

Remark 7. To show that the estimator/controller structure is able to control the surface roughness independent of the

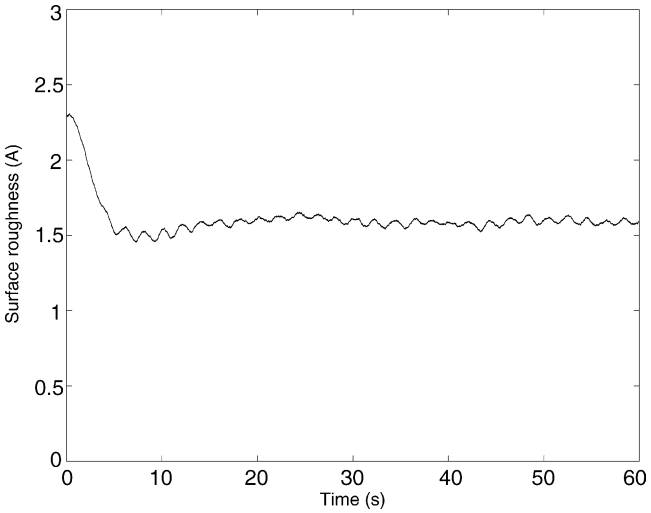

Fig. 14. Evolution of the surface roughness under feedback control based on the roughness estimator – delayed roughness measurements.

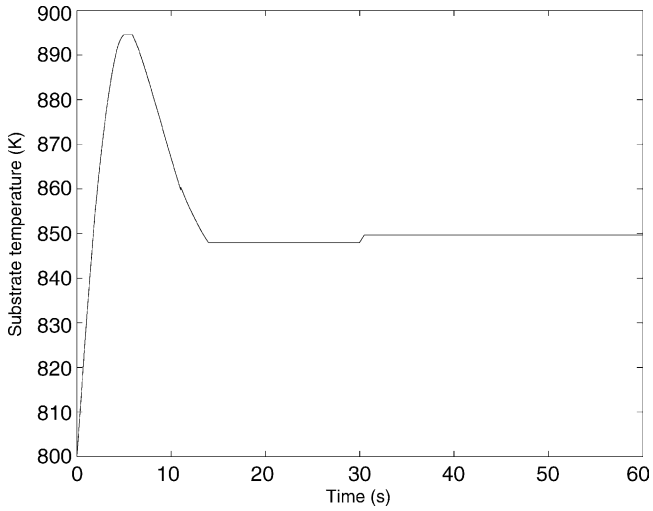

Fig. 15. Evolution of the substrate temperature under feedback control based on the roughness estimator – delayed roughness measurements.

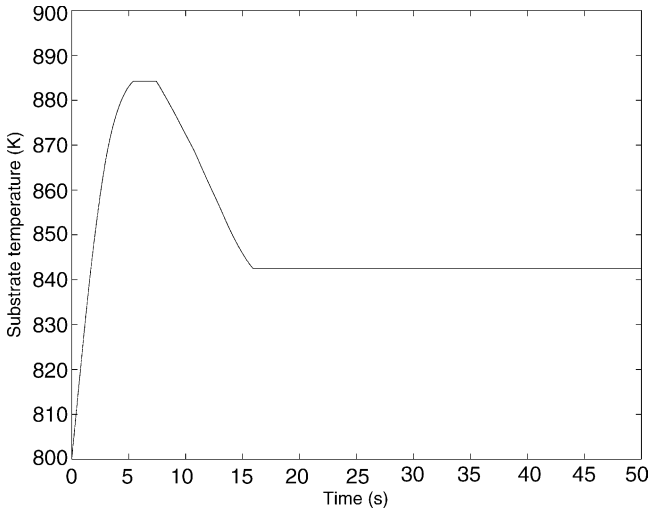

Fig. 17. Evolution of the substrate temperature under open-loop implementation of the estimator/controller structure.

frequency at which the roughness measurements are available, the developed estimator/controller structure was implemented without using roughness measurements, i.e. the controller determines the substrate temperature based only on the output of the kinetic MC simulator which uses six small-lattice models and the adaptive filter. Figs. 16 and 17 show the resulting profiles of surface roughness and substrate temperature, respectively. The simulation results show that this open-loop implementation of the controller/estimator structure (with parameters shown in Table 3) successfully drives the surface roughness to the desired level.

Remark 8. Note, although we demonstrate the effectiveness of the estimator/controller structure by applying it to a kMC process model using a large lattice, the results obtained from our numerical simulations are indicative of the application of the proposed estimator/controller structure to actual GaAs MOCVD processes. The reasons are: (1) the kMC model is validated by using experimental data and (2) the estimator/controller structure has very good robustness properties with respect to significant model parameter uncertainty, therefore, the presence of unmodeled dynamics in an experimental setting would not significantly deteriorate the closed-loop performance.

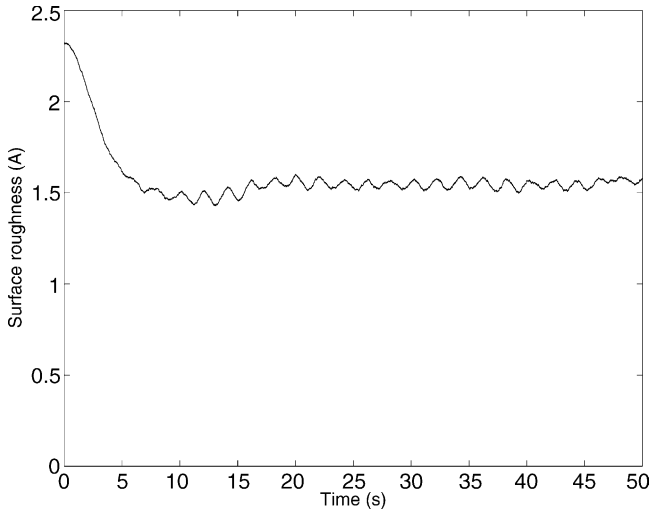

Fig. 16. Evolution of the surface roughness under open-loop implementation of the estimator/controller structure.

6. Conclusions

In this study, the methodology presented in Lou and Christofides (2003a) was used to study estimation and control of surface roughness of GaAs (0 0 1) thin films during deposition in a horizontal-flow quartz reactor using TIBGa and TBAs as precursors and H_2 as the carrier gas. The adsorption of TIBGa onto the surface and the migration of Ga atoms on the surface were considered as the two rate-limiting steps in the film growth and were explicitly modeled within a kinetic Monte Carlo simulation framework. The energy barrier and the pre-exponential factor of the migration rate of Ga atoms on the surface used in the simulations were initially determined by fitting the simulation results to experimental data reported in Law et al. (2000). Then, a roughness estimator was constructed that provided estimates of the surface roughness of the GaAs thin films at a time-scale comparable to the real-time evolution of the process using discrete on-line roughness measurements. The estimator involves a kinetic MC simulator based on multiple small-lattice models, an adaptive filter used to reduce roughness stochastic fluctuations and an error compensator used to reduce the error between the roughness estimates and the roughness measurements. The roughness estimates are then used as input to a PI feedback controller that controls the surface roughness to a desired level by manipulating the substrate temperature. Application

of the proposed estimator/controller structure to the process model based on a large-lattice kinetic Monte Carlo simulator demonstrated successful control of the surface roughness. The proposed approach was shown to be superior to only PI control with direct use of the measured discrete roughness. The reason being that the available measurement techniques do not provide measurements at a frequency that is comparable to the time-scale of evolution of the dominant film growth dynamics.

Acknowledgement

Financial support from the NSF (ITR), CTS-0325246, is gratefully acknowledged.

References

Armaou, A., & Christofides, P. D. (1999). Plasma-enhanced chemical vapor deposition: modeling and control. *Chemical Engineering Science*, *54*, 3305–3314.

Baker, J., & Christofides, P. D. (1999). Output feedback control of parabolic PDE systems with nonlinear spatial differential operators. *Industrial & Engineering Chemistry Research*, *38*, 4372–4380.

Baker, J., & Christofides, P. D. (2000). Finite dimensional approximation and control of nonlinear parabolic PDE systems. *International Journal of Control*, *73*, 439–456.

Blakemore, J. S. (1982). Semiconducting and other major properties of gallium arsenide. *Journal of Applied Physics*, *53*, R123–R181.

Christofides, P. D. (2001). *Nonlinear and robust control of PDE systems: methods and applications to transport-reaction processes*. Boston, MA: Birkhäuser.

Christofides, P. D., & Daoutidis, P. (1997). Finite-dimensional control of parabolic PDE systems using approximate inertial manifolds. *Journal of Mathematical Analysis and Applications*, *216*, 398–420.

Cui, J., Ozeki, M., & Ohashi, M. (1998). Dynamical approach to the surface reaction of triisobutylgallium (TIBGa) on GaAs(0 0 1) by using molecular beam scattering. *Journal of Crystal Growth*, *188*, 137–143.

Curtis, R., Mitsui, T., & Ganz, E. (1997). An ultrahigh vacuum high speed scanning tunneling microscope. *Review of Scientific Instruments*, *68*, 2790–2796.

Feller, W. (1975). *An introduction to probability theory and its applications*. New York: Wiley.

Fichthorn, K. A., & Weinberg, W. H. (1991). Theoretical foundations of dynamical Monte Carlo simulations. *Journal of Chemical Physics*, *95*, 1090–1096.

Fu, Q., Li, L., & Hicks, R. F. (2000). Ab initio cluster calculations of hydrogenated GaAs(0 0 1) surfaces. *Physical Review B*, *61*, 11034–11040.

Gallivan, M. A., & Murray, R. M. (2003). Model reduction and system identification of master equation control systems. *Proceedings of American Control Conference Denver, CO*. 3561–3566.

Gillespie, D. T. (1976). A general method for numerically simulating the stochastic time evolution of coupled chemical reactions. *Journal of Computational Physics*, *22*, 403–434.

Gillespie, D. T. (1977). Exact stochastic simulation of coupled chemical reactions. *The Journal of Physical Chemistry*, *81*, 2340–2361.

Gillespie, D. T. (1992). A rigorous derivation of the chemical master equation. *Physica A*, *188*, 404–425.

Granneman, E. H. (1993). Thin films in the integrated circuit industry: requirements and deposition methods. *Thin Solid Films*, *228*, 1–11.

Heyn, C., Franke, T., & Anton, R. (1999). Modelling of compound semiconductor epitaxy. *Journal of Crystal Growth*, *201*, 67–72.

Ishii, A., & Kawamura, T. (1999). Monte Carlo simulation of homoepitaxial growth on two-component compound semiconductor surfaces. *Surface Science*, *436*, 38–50.

Ito, T., & Shiraishi, K. (1996). A Monte Carlo study on the structural change of the GaAs(0 0 1) surface during MBE growth. *Surface Science*, *357*, 486–489.

Itoh, M., Bell, G. R., Joyce, B., & Vvedensky, D. (2000). Transformation kinetics of homoepitaxial islands on GaAs(0 0 1). *Surface Science*, *464*, 200–210.

Kasu, M., & Kobayashi, N. (1997). Surface kinetics of metalorganic vapor-phase epitaxy: surface diffusion, nucleus formation, sticking at steps. *Journal of Crystal Growth*, *174*, 513–521.

Lam, R., & Vlachos, D. G. (2001). Multiscale model for epitaxial growth of films: growth mode transition. *Physical Review B*, *64*, 035401.

Law, D. C., Li, L., Begarney, M. J., & Hicks, R. F. (2000). Analysis of the growth modes for gallium arsenide metalorganic vapor-phase epitaxy. *Journal of Applied Physics*, *88*, 508–512.

Lou, Y., & Christofides, P. D. (2003). Estimation and control of surface roughness in thin-film growth using kinetic Monte-Carlo models. *Chemical Engineering Science*, *58*, 3115–3129.

Lou, Y., & Christofides, P. D. (2003). Feedback control of growth rate and surface roughness in thin-film growth. *AIChE Journal*, *49*, 2099–2113.

Melsa, J. L., & Sage, A. P. (1973). *An introduction to probability and stochastic processes*. Englewood Cliffs, NJ: Prentice-Hall.

Meng, B., & Weinberg, W. H. (1996). Dynamical Monte Carlo studies of molecular beam epitaxial growth models: interfacial scaling and morphology. *Surface Science*, *364*, 151–163.

Ni, D., Lou, Y., Christofides, P. D., Sha, L., Lao, S., & Chang, J.P. (2004). Real-time carbon content control for PECVD ZrO_2 thin-film growth. *IEEE Transactions on Semiconductor Manufacturing*, 17, 221–230.

Palasantzas, G. (1993). Roughness spectrum and surface width of self-affine fractal surfaces via the K-correlation model. *Physical Review B*, *48*, 14472–14478.

Reese, J. S., Raimondeau, S., & Vlachos, D. G. (2001). Monte Carlo algorithms for complex surface reaction mechanisms: efficiency and accuracy. *Journal of Computational Physics*, *173*, 302–321.

Shiraishi, K. (1996). First-principles calculations of surface adsorption and migration on GaAs surfaces. *Thin Solid Films*, *272*, 345–363.

Shiraishi, K. (2001). Monte Carlo simulation of recovery process after MBE growth on GaAs(1 0 0). *Surface Science*, *493*, 438–446.

Shitara, T., Vvedensky, D. D., Wilby, M. R., Zhang, J., Neave, J. H., & Joyce, B.A. (1992a). Misorientation dependence of epitaxial growth on vicinal GaAs(0 0 1). *Physical Review B*, *46*, 6825–6833.

Shitara, T., Vvedensky, D. D., Wilby, M. R., Zhang, J., Neave, J. H., & Joyce, B. A. (1992). Step-density variations and reflection high-energy electron-diffraction intensity oscillations during epitaxial growth on vicinal GaAs(0 0 1). *Physical Review B*, *46*, 6815–6824.

Siettos, C. I., Armaou, A., Makeev, A. G., & Kevrekidis, I. G. (1922). Microscopic/stochastic timesteppers and "coarse" control: a kMC example. *AIChE Journal*, *49*, 1922–1926.

Sinha, S. K., Sirota, E. B., Garoff, S., & Stanley, H. B. (1988). X-ray and neutron scattering from rough surfaces. *Physical Review B*, *38*, 2297–2311.

Tanenbaum, D. M., Laracuente, A. L., & Gallagher, A. (1997). Surface roughening during plasma-enhanced chemical-vapor deposition of hydrogenated amorphous silicon on crystal silicon substrates. *Physical Review B*, *56*, 4243–4250.

Tejedor, P., Šmilauer, P., Roberts, C., & Joyce, B. A. (1999). Surface-morphology evolution during unstable homoepitaxial growth of GaAs(1 1 0). *Physical Review B*, *59*, 2341–2345.

Theodoropoulou, A., Adomaitis, R. A., & Zafiriou, E. (1999). Inverse model based real-time control for temperature uniformity of RTCVD. *IEEE Transactions on Semiconductor Manufacturing*, *12*, 87–101.

Tirtowidjojo, M., & Pollard, R. (1988). Elementary processes and rate-limiting factors in MOVPE of GaAs. *Journal of Crystal Growth*, *93*, 108–114.

Van Kampen, N. G. (1992). *Stochastic processes in physics and chemistry*. Amsterdam: North-Holland.

Vanhove, J. M., Lent, C. S., Pukite, P. R., & Cohen, P. I. (1983). Damped oscillations in reflection high-energy electron-diffraction during GaAs MBE. *Journal of Vacuum Science and Technology B, 1*, 741–746.

Vlachos, D. G. (1997). Multiscale integration hybrid algorithms for homogeneous–heterogeneous reactors. *AIChE Journal*, *43*, 3031–3041.

Voigtländer, B. (2001). Fundamental processes in Si/Si and Ge/Si studied by scanning tunneling microscopy during growth. *Surface Science Reports*, *43*, 127–254.